As a final point we note that Scheme I increases the fraction of reversed units in PVF_2 because the comonomer unit is attacked by the growing VF_2 radical (which has the $-CH_2-CF_2\cdot$ orientation[6]) at the CF_2 carbon and not the CFX carbon. Presumably this occurs to minimize steric and electrostatic repulsion forces which are accentuated by the bulky X halogen. Clearly this scheme can be made more general by the appropriate choice of comonomer pairs, and we are presently examining its utility for preparing highly aregic poly(vinyl fluoride) and poly(trifluoroethylene) as well.

Acknowledgment. We are grateful to Dr. A. J. Lovinger for recording and interpreting X-ray diffraction photographs and to Dr. P. Mirau for assistance with the NMR experiments.

Registry No. (VF_2) (homopolymer), 24937-79-9.

References and Notes

(1) Bovey, F. A. "Chain Structure and Conformation of Macromolecules"; Academic Press: New York, 1982; Chapter 6.
(2) Koenig, J. L. "Chemical Microstructure of Polymer Chains"; Wiley-Interscience: New York, 1980; pp 288–292.
(3) Görlitz, M.; Minke, R.; Trautvetter, W.; Weisgerber, G. *Angew. Makromol. Chem.* **1973**, *29/30*, 137–162.
(4) Lando, J. B.; Doll, W. W. *J. Macromol. Sci., Phys.* **1968**, *B2*, 205–218.
(5) Farmer, B. L.; Hopfinger, A. J.; Lando, J. B. *J. Appl. Phys.* **1972**, *43*, 4293–4303.
(6) Cais, R. E.; Kometani, J. M. *Macromolecules* **1984**, *17*, 1887–1889.
(7) Cais, R. E.; Kometani, J. M. *Org. Coat. Appl. Polym. Sci. Proc. Am. Chem. Soc.* **1983**, *48*, 216–220.
(8) Bax, A. "Two-Dimensional Nuclear Magnetic Resonance in Liquids"; Delft University Press and D. Reidel Publishing Co.: Dordrecht, Netherlands, 1982.
(9) Wider, G.; Macura, S.; Kumar, A.; Ernst, R. R.; Wutrich, K. *J. Magn. Reson.* **1984**, *56*, 207–234.
(10) Ferguson, R. C.; Ovenall, D. W. *Polym. Prepr., Am. Chem. Soc., Div. Polym. Chem.* **1984**, *25* (1), 340–341.
(11) Bruch, M. D.; Bovey, F. A.; Cais, R. E. *Macromolecules* **1984**, *17*, 2547–2551.
(12) Cais, R. E.; Kometani, J. M. *Macromolecules* **1984**, *17*, 1932–1939.
(13) Kobayashi, M.; Tashiro, K.; Tadokoro, H. *Macromolecules* **1975**, *8*, 158–171.
(14) Cais, R. E.; Sloane, N. J. A. *Polymer* **1983**, *24*, 179–187.
(15) Cais, R. E.; Kometani, J. M., to be published.
(16) Ferguson, R. C.; Brame, E. G. *J. Phys. Chem.* **1979**, *83*, 1397–1401.
(17) Tonelli, A. E.; Schilling, F. C.; Cais, R. E. *Macromolecules* **1982**, *15*, 849–853.
(18) We have prepared an oligomer containing alternating ethylene and tetrafluoroethylene units (equivalent to syndioregic PVF_2). The fluorine-19 chemical shift (in dimethylformamide at 160 °C) was −114 ppm.
(19) Lovchikov, V. A.; Shylakov, A. M.; Doglopolskii, I. M. *Issled. Str. Makromol. Metodom YAMR Vysok. Razresh., M.* **1983**, 51–62.

Rudolf E. Cais* and Janet M. Kometani
AT&T Bell Laboratories
Murray Hill, New Jersey 07974

Received March 15, 1985

Accurate Lattice Constants for Tara Gum

Tara gum, obtained from the seed endosperm of *Caesalpinia spinosa*, is a galactomannan of the same general structure as guar and locust bean or carob gums.[1] As such, it has a linear 1→4-linked main chain of β-D-mannose with α-D-galactosyl substituents linked 1→6 to about one-third of the mannose residues. The structure is best represented by a mannobiose repeat in the main chain with variable mole fractions of galactose, x_i and x_j, attached to the adjacent mannose residues i and j; see Figure 1. The sum of x_i and x_j should equal twice the galactose substitution or DS. In this model regular alternation of substituted and free mannosyl residues as was originally proposed for guar[2] would take the form $x_i = 2$(DS) and $x_j = 0$. A truly random arrangement would take the form $x_i = x_j =$ DS and irregular distributions of the type now most widely believed to exist[3] could have any value of x_i and x_j subject to the constraint on their sum.

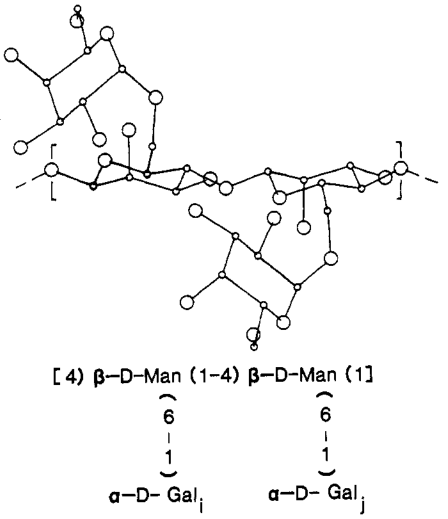

Figure 1. Generalized primary structure model for the crystallographic repeat of a galactomannan such as tara gum. Symbols Gal$_i$ and Gal$_j$ denote D-galactose residues of mole fractions x_i and y_i attached to residues i and j of the poly[(1→4)-β-D-mannose] chain.

Commercially, galactomannans are of importance in a diversity of applications because of the precise control over hydrorheology which they offer. The galactomannans and their parent compound mannan also present interesting structural problems in the attempt to correlate galactose content and distribution with molecular interactions and hydrodynamic properties.[3] In this context the simplest model to consider is the effect of galactose content on self-association in crystalline domains. Our laboratory is currently making a survey of several galactomannans and the initial diffraction data for one of these, tara gum, is the subject of this communication.

Materials and Methods. The original material was a gift from Dr. Gordon C. Towle of Celanese Corp. This material was precipitated from water with 95% ethanol, dissolved in water, and dialyzed exhaustively against water at 4 °C before lyophilization and storage. Samples were redissolved in water after grinding with a mortar and pestle at liquid nitrogen temperatures and 1% solutions were dried on Teflon blocks into clear, tough films. The water used in all procedures was glass distilled. Small (2 mm × 8 mm) pieces of these films were glued on to plastic supports and then suspended under a load of 10–20 g while being stored at 95% relative humidity and 50 °C. After 24 h they had extended to 300% of their initial length. The resulting films were highly birefringent as evidenced by their sharp extinction upon rotation between crossed polarizers in the polarizing microscope. These films were annealed by heating them to 105–115 °C in a sealed container with a small amount of water. X-ray diffraction data was collected at 81% relative humidity and room temperature using nickel-filtered Cu Kα radiation from a Philips sealed-tube generator. Diffraction patterns were recorded on Kodak No-Screen film.

Results and Discussion. The X-ray diffraction pattern

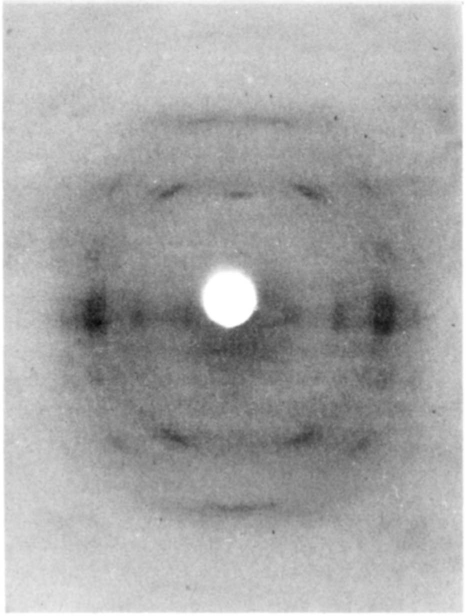

Figure 2. Typical X-ray diffraction pattern for tara gum at 81% relative humidity and room temperature. The specimen was dusted with calcite (characteristic spacing 3.035 Å) and tilted by 10° from the normal to the incident beam during the exposure.

typical of tara gum is shown in Figure 2. This pattern may be indexed on the basis of an orthohombic unit cell with $a = 8.91$ (3), $b = 24.17$ (10), and c (fiber repeat) = 10.46 (4) Å using 24 observed reflections. The agreement between observed and calculated spacings is better than 99%. A probable space group is $P2_12_12$ and is supported by the absence of only odd-order $h00$ and $0k0$ reflections. Density considerations together with the space group symmetry require that four chains with a total of eight mannosyl residues pass through this unit cell. The parent mannan structure has $P2_12_12_1$ symmetry,[4] and the fiber axis coincides with one set of screw dyads parallel to c. However, this relationship cannot persist if either the geometry or the mole fraction of galactose differs on adjacent sites. With tara there are eight mannosyl residues per unit cell and only four can be related by the space group symmetry irrespective of whether the symmetry axes parallel to c are thought to be 2-fold rotation or screw axes. Since 003 relfections of medium to medium weak intensity are found in all the diffraction patterns which we have examined, we favor the rotation axis assumption. It should be noted, however, that even if these reflections should prove to be aritifacts arising from small crystallite size, the adoption of a model with screw axes parallel to c does not establish the existence of a molecular 2_1 helix axis. The same space group also has been proposed for guar,[5] where the meridional intensity for 0,0,odd reflections is even more apparent.

The feature of particular interest in this pattern is that despite the distinctly different galactose content of tara as compared to either mannan or guar, two of the three lattice dimensions remain relatively constant. In mannan I from several sources the a dimensions is 8.92 Å[4] and the fiber repeat is 10.27 Å,[6] while in guar the corresponding values are 9.09 and 10.22 Å, respectively.[5] Additional experiments on a variety of enzymatically degalactosylated guars show this result to be ubiquitous for a wide range of galactomannans.[7]

The obvious interpretation to this result is that the mannan chains must be organized into a lamellar structure held together by mannan–mannan interactions in the ac plane and largely identical with those in the native mannan I structure. The galactose side chains must then protrude from either side of this sheet. As the degree of galactose substitution on mannose increases from a minimum value of zero in mannan to about every third residue in tara and every second mannose residue in guar, the restrictions imposed by galactose–galactose interactions along the same chain become more severe. Given the constancy of the fiber repeat, these interactions can be resolved by having the galactose residues become more nearly perpendicular to the fiber direction. For this reason the third dimension of the crystal structure should increase with increasing galactose content even though the available chemical evidence is that all of the galactose occurs as monomeric substitutents on the mannan chain.[8] Alternative hypotheses involving the incorporation of chemically different regions of the D-galacto-D-mannan molecule regularly distributed in the unit cell or major orientational differences between symmetry-independent chains have been proposed on the basis of similar X-ray results.[9] The first of these arguments would require an extremely precise recognition between mannan and galactomannans, for which there is, as yet, no experimental evidence. The possibility of orientational differences is also consistent with the present model.

If one measures the line broadening of reflections close to the meridian on the tara diffraction pattern, they can provide, through the Scherrer equation,[10] an indication of the size of the crystalline domains in the fiber axis direction. The result of this calculation for the tara data suggests a crystallite length of 10 nm. This calculation does not allow for the the additional line broadening arising from defects and the value is, therefore, a lower limit to the crystallite size in the fiber axis direction. Since the main-chain conformation is essentially that of mannan I or cellulose, this corresponds to 19 mannose residues. If we accept the prevailing model of a nonregular distribution of galactose on the mannan chain with some tendency toward the occurrence of substituted doublets,[11] then it becomes clear that the crystallite is far too large to involve association of domains of mannan with periodic galactose substitution on alternate units. Alternatively, if the repeating motif involves some unit larger than the mannobiose segment, we would expect a change in the fiber repeat and a concomitant change in the layer line spacing in the diffraction pattern. No such alteration is observed in any of our diffraction data. Finally, exclusion of the aperiodic domains from the structure should also give rise to a strong amorphous halo and this is not observed in our data. Distinguishing between adjacent mannose residues in a chain as in Figure 1, galactose attached to adjacent mannose residues will be in distinctively different packing environments and the relative amount in each site should affect the intensity distribution in a determinable fashion. Further studies of guar, tara, and other galactomannans are in progress to more fully establish how all galactomannans are simply variations upon the mannan structural theme.

Acknowledgment. Support by the donors of the Petroleum Research Fund, administered by the American Chemical Society, is gratefully acknowledged. W.T.W. thanks his hosts and colleagues at the Centre de Recherches sur les Macromolécules Végétales (CERMAV, CNRS), St. Martin d'Heres, France, for their hospitality and constructive discussions during the writing of the manuscript.

References and Notes

(1) Dea, I. C. M.; Morrison, A. *Adv. Carbohydr. Chem. Biochem.* **1975**, *31*, 241.

(2) Whistler, R. L.; Smart, C. L. "Polysaccharide Chemistry"; Academic Press: New York, 1959; pp 296–300.

(3) McCleary, B. V.; Dea, I. C. M.; Clark, A. H. In "Gums and Stabilisers for the Food Industry 2"; Philips, G. O., Wedlock, D. J., Williams, D. A., Eds.; Pergamon: Oxford, 1984; p 33.

(4) Chanzy, H.; Dube, M.; Marchessault, R. H. *Biopolymers* **1979**, *18*, 887.

(5) Winter, W. T.; Bouckris, H.; Chien, Y. Y.; Okuyama, K.; Arnott, S. *J. Mol. Biol.*, submitted.

(6) Nieduszynski, I.; Marchessault, R. H. *Can. J. Chem.* **1977**, *50*, 2130.

(7) Winter, W. T.; Bouckris, H.; Chien, Y. Y.; Okuyama, K.; Taravel, F. R.; Arnott, S., in preparation.

(8) Rafique, C. M.; Smith, F. *J. Am. Chem. Soc.* **1950**, *72*, 4634.

(9) Marchessault, R. H.; Buléon, A.; Deslandes, Y.; Goto, T. *J. Colloid Interface Sci.* **1979**, *71*, 375.

(10) Alexander, L. E. "X-Ray Diffraction Methods in Polymer Science"; Wiley: New York, 1969; p 423.

(11) (a) McCleary, B. V.; Matheson, N. K. *Carbohydr. Res.* **1983**, *119*, 191. (b) Painter, T. J.; Gonzalez, J. J.; Hemmer, P. C. *Carbohydr. Res.* **1979**, *69*, 217.

Y. Y. Chien and William T. Winter*

Department of Chemistry and
Polymer Research Institute
Polytechnic Institute of New York
Brooklyn, New York 11201

Received January 22, 1985

Melt Properties of Ring Polystyrenes[†]

Recently, narrow molecular weight distribution ring polystyrenes with molecular weights between 7000 and 450 000 have been prepared and characterized and some of their dilute solution properties have been described.[1,2] As an example of the purity of the ring polymers, the sedimentation boundaries of a ring polymer (R19D) and a synthetic mixture of the ring and its linear precursor are compared in Figure 1. There is presently speculation about the melt properties of large entangled rings because neither the reptation mechanism of linear polymers nor the chain retraction prominent in star polymers is expected to be effective in rings. Indeed, both relaxation mechanism require the existence of chain ends. The melt viscosities of unentangled low molecular weight poly(dimethylsiloxane) rings are approximately half those of linear polymers,[3] in agreement with the modified Rouse normal mode analysis.[4]

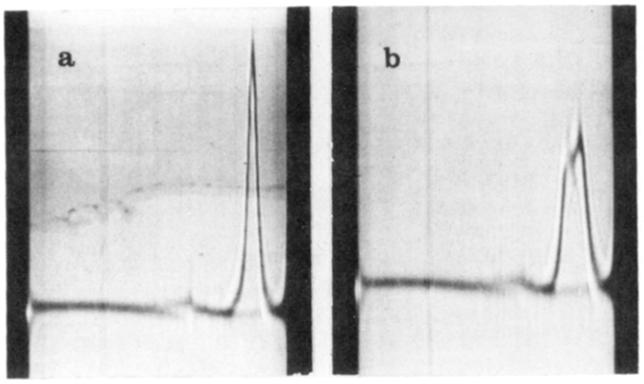

Figure 1. (a) Ultracentrifugation boundary of ring polystyrene R19D in cyclohexane at 35 °C and 60 000 rpm. Sedimentation from left to right. (b) Same as (a) for a synthetic mixture of R19D and 20% linear percursor. Due to the Johnston–Ogston effect the slower sedimenting 20% linear polymer appears as almost 50% of the total.

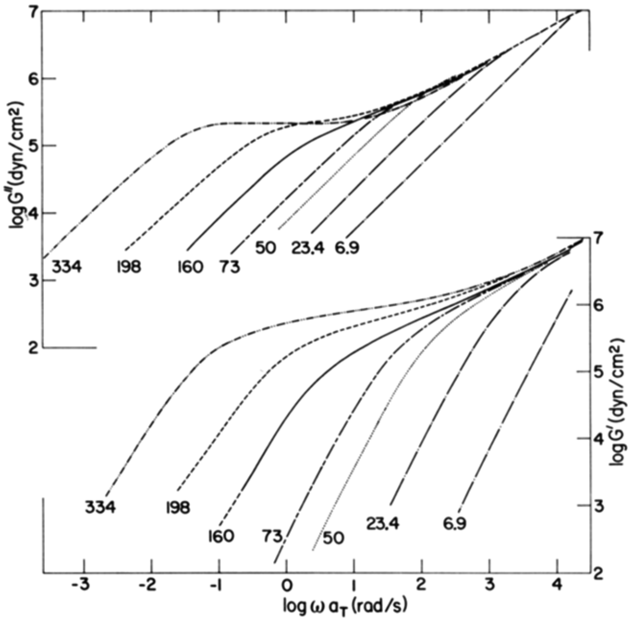

Figure 2. Moduli–frequency master curves for the ring polymers at T_r = 169.5 °C. Numbers indicate molecular weight (×10^{-3}) of the polymers.

The glass transition temperature (T_g) of the rings was measured with a Du Pont 1090 thermal analyzer in the DSC mode. The heating rate was 10 °C/min. In Table I, $\Delta T_g = T_g(\infty) - T_g$ is given, where $T_g(\infty)$ is the high molecular weight limit of T_g. The experimental $T_g(\infty)$ for ring and linear polystyrene is the same. The true glass transition temperature of polystyrene was taken equal to 100 °C. From Table I it can be seen that the dependence of ΔT_g on molecular weight is less for rings than for linear polymers. This is in qualitative agreement with the hypothesis that T_g is inversely proportional to the chain-end concentration.[5] The reason for the residue decrease of T_g with decreasing molecular weight of the rings is not known.

The storage (G') and loss (G'') moduli of the melts were measured with a Rheometrics mechanical spectrometer in the dynamic mode. Measurements as a function of frequency (ω) were made at temperatures between T_g + 40 °C and T_g + 110 °C. Master curves at the reference temperature T_r = 169.5 °C were constructed by horizontally shifting the moduli–frequency curves at the other temperatures by a_T. Master curves are shown in Figure 2. Vertical shifts smaller than $(\rho_r T_r)/(\rho T)$, where ρ is the density of the melt, were only applied above T_g + 90 °C. No evidence of degradation during melt measurements was found by GPC. The observed zero-shear viscosities, $\eta_0 = \lim_{\omega \to 0} (G''/\omega)$, of the ring and linear polymers at T_r are given in Table I and plotted double-logarithmically against M_w on the left-hand side of Figure 3. Except for the low molecular weight ring, η_0 of the rings is less than that of the linear polymers. The isothermal data were converted to iso-free volume data. The temperature dependence of η_0 and a_T was found to be given by $\log a_T = \log \eta_0 = B/[2.303\alpha_f(T - T_0)]$.[6] The slopes of plots of $\log a_T$ vs. $1/(T - T_0)$, where T_0 and T_g − 55 °C, gave 764 ± 15 K for all linear and ring polymers except PS10 and PS5. With B = 1, α_f, the thermal expansion coefficient of the fractional free volume, is 5.7×10^{-4} K^{-1}, in good agreement with published data.[7,8] Zero-shear viscosities at T_g + 69.5 °C (fractional free volume f = 0.071) are also given in Table I. For PS10, $T_0 = T_g - 51.5$ °C, $\alpha_f = 5.95 \times 10^{-4}$, and f = 0.071 at 158.4 °C. For PS5, $T_0 = T_g - 45.3$ °C, $\alpha_f = 6.4 \times 10^{-4}$, and f = 0.071 at 147.7 °C. From the right-hand side of Figure 3 it can be seen that for linear polystyrene under iso-free volume conditions $\eta_0 \propto M_w$ below M_w = 38 000 and $\eta_0 \propto M_w^{3.4}$ above 38 000. For the rings, values

---

[†] Issued as NRCC No. 24347.